3-30-2012

Characterization of Species C Human Adenovirus Serotype 6 (Ad6)

Eric A. Weaver

Reeti Khare

Mathew L. Hillestad

Donna Palmer

Philip Ng

See next page for additional authors

Authors
Eric A. Weaver, Reeti Khare, Mathew L. Hillestad, Donna Palmer, Philip Ng, and Michael A. Barry

Published in final edited form as:
Virology. 2011 March 30; 412(1): 19–27. doi:10.1016/j.virol.2010.10.041.

Characterization of Species C Human Adenovirus Serotype 6 (Ad6)

Eric A. Weaver[1], **Reeti Khare**[2], **Mathew L. Hillestad**[2], **Donna Palmer**[3], **Philip Ng**[3], and **Michael A. Barry**[1,4]

[1] Division of Infectious Diseases, Department of Internal Medicine, Translational Immunovirology and Biodefense Program, Mayo Clinic, Rochester, MN 55902

[2] Virology and Gene Therapy Graduate Program, Mayo Graduate School, Mayo Clinic, Rochester, MN 55902

[3] Department of Molecular and Human Genetics, Baylor College of Medicine, 1 Baylor Plaza, Houston, TX 77030, USA

[4] Department of Immunology, Department of Molecular Medicine[4], Mayo Clinic, Rochester, MN 55902

Abstract

Adenovirus serotype (Ad5) is the most studied Ad. Ad1, 2, and 6 are also members of species C Ad and are presumed to have biologies similar to Ad5. In this work, we have compared the ability of Ad1, 2, 5, and 6 to infect liver and muscle after intravenous and intramuscular injection. We found that Ad6 was surprisingly the most potent at liver gene delivery and that Ad1 and Ad2 were markedly weaker than Ad5 and 6. To understand these differences, we sequenced the Ad6 genome. This revealed that the Ad6 fiber protein is surprisingly three shaft repeats shorter than the others which may explain differences in virus infectivity *in vitro*, but not in the liver. Comparison of hexon hypervariable regions (HVRs) suggests that the higher transduction by Ad5 and 6 as compared to Ad1 and 2 may be related to differences in charge and length.

Introduction

There are currently 55 serotypes of adenoviruses (Ads) that infect humans. Ad serotype 5 (Ad5) is the most studied Ad given its early isolation, efficient reverse genetic systems, and its use as a gene therapy and vaccine vector. While Ad5 is well studied, it is arguably one of the worst Ads for use in humans due to rampant pre-existing immunity in humans to this virus. Depending on the study 25–100% of the population has been exposed to Ad5 (Abbink et al., 2007; Piedra et al., 1998). This high level of pre-existing antibodies to Ad5 will likely lead to vector neutralization upon administration into most human patients.

Given this, recent efforts have been directed at identifying and developing other Ad serotypes with lower seroprevalence in humans (Lemckert et al., 2005; Vogels et al., 2003). The seroprevalence of Ad6 is lowest of the subgroup C viruses. In children in Italy, Ad5 and

Correspondence to: Michael A. Barry, Ph.D., Mayo Clinic, 200 First Street SW Rochester, MN, 55902, Tel: 507-266-9090, Fax: 507-255-2811, mab@mayo.edu.

Ad6 seroprevalence was 32 and 15%, respectively (D'Ambrosio et al., 1982). The seroprevalence of Ad5 and Ad6 was approximately 78% and 44% in healthy Belgian adults (Vogels et al., 2003). In the United States, Ad5 seroprevalence in healthy adults was reported at 27.3% and 3% for Ad6 based on neutralization (Piedra et al., 1998). These variations may be related to differences in location or due to the conditions and thresholds at which samples are considered positive.

Unlike other species C viruses, Ad6 is rarely detected in human lymphoid tissues. For example, when 103 species C-positive tonsil and adenoid tissues were assayed by serotype-specific PCR, Ad1, 2, and 5 were detected 25, 30, and 24 times (Garnett et al., 2009). In contrast, Ad6 was detected 3 times. Therefore, Ad6 is the least prevalent species C virus in humans.

Recently, Ad6 has been tested as a lower seroprevalence vector for gene-based vaccines and oncolytic virotherapy (Capone et al., 2006; Senac et al., ; Shashkova, May, and Barry, 2009; Weaver et al., 2009a; Weaver et al., 2009b). In these applications, Ad6 appears nearly as potent as Ad5 for vaccine (Weaver et al., 2009a) and is as good or better than Ad5 for solid tumor cell killing (Shashkova, May, and Barry, 2009). Given these observations and its lower seroprevalence, we have compared the pharmacology of Ad6 after intravenous and intramuscular injection to Ad1, Ad2, and Ad5. We have also sequenced the full viral genome and have performed sequence comparisons with other species C Ads to explore how differences in key proteins might explain substantial differences in virus pharmacology after intravenous injection.

Materials and Methods

Adenoviruses

Human Ad6 (Tonsil 99) was obtained from ATCC and was purified by CsCl-banding. Helper-Dependent (HD)-Ad viruses expressing the green fluorescent protein-luciferase fusion protein (GFPLuc) were produced as previously described (Weaver et al., 2009a). Each HD-Ad plasmid backbone was cut with Pme I and 10 μg of the genome was transfected into a 60 mm plate of Cre-expressing 116 cells (Palmer and Ng, 2003). One day later, Ad5 helper virus AdNG163 (Palmer and Ng, 2003) was used to rescue HD-Ad. Lysates were then serially passaged up to a 3 liter culture and virus was purified by CsCl banding (Palmer and Ng, 2003). HD-Ad1, 2, and 6 vectors were produced similarly by infection with HD-Ad1, 2, or 6 helper viruses Ad1LC8cCEVS-1, Ad2LC8cCARP (Parks, Evelegh, and Graham, 1999), and Ad6LC8cCEVS-1 (provided by Carole Evelegh and Frank L. Graham (McMaster University)) as in (Weaver et al., 2009a).

Animals

Female BALB/c mice (6–8 weeks old) were purchased from Charles River Laboratories (Wilmington, Massachusetts, USA) and housed in the Mayo Clinic Animal Facility under the Association for Assessment and Accreditation of Laboratory Animal Care (AALAC) guidelines with animal use protocols approved by the Mayo Clinic Animal Use and Care Committee. All animal experiments were carried out according to the provisions of the Animal Welfare Act, PHS Animal Welfare Policy, the principles of the NIH Guide for the Care and Use of Laboratory Animals, and the policies and procedures of Mayo Clinic. Mice injected intramuscularly (i.m.) received 1×10^{10} vp/mouse in 50 μl. Mice injected intravenously (i.v.) received 1×10^{10} vp/mouse in 100 μl by tail vein injection.

Luciferase Imaging of Mice

Molecular light imaging of luciferase *in vivo* was accomplished using a Lumazone imaging system (Roper Scientific). At indicated days post- injection, mice were anesthetized with Isoflurane, injected i.p. with d-luciferin at a concentration of 20 mg/ml in PBS in a volume of 200 μl and the mice were immediately placed into the Lumazone Imager and images were captured. All images were taken with a 10 minute exposure and 4 × 4 binning using no filters and no photo-multiplication. Data analysis was performed on each image using background subtracted mean intensities detected by the Lumazone Imaging Software at each time point and graphed using Prism Graphing Software

Factor X–dependent Virus Binding and Transduction

Human HepG2 and SKOV-3 cells were cultured in complete Dulbecco's Modified Eagle's Medium (cDMEM) that contained 10% heat-inactivated fetal calf serum (Gibco, Aukland, NZ) and penicillin/streptomycin at 100 U/ml (Gibco, Aukland, NZ). For transgene expression, SKOV-3 and HepG2 cells were plated at 2×10^4 cells/well into 96- black plates (3603 Corning). Viruses were diluted to a final concentration of 2×10^8 vp/ml in cDMEM containing 8 μg/ml FX (Haematologic Technologies Inc., Essex Junction, Vermont, USA) and 100 μl was added per well. Virus and cells were maintained at 37°C for 3 hours. Cells were washed twice with 200 μl of cDMEM and 100 μl of cDMEM was added to each well. Cells were maintained at 37°C until harvesting at 72 hours. Cells were lysed by the addition of 25 μl of 5X Passive Lysis Buffer (Promega Corporation, Madison, WI, USA) and 50 μl of Luciferase Assay Reagent (Promega Corporation, Madison, WI, USA) was added. Luminescence was measured using a Beckman Coulter DTX 880 Multimode Detector as in (Hofherr et al., 2008). Cell binding experiments were performed using HepG2 cells in 12-well plates. Viruses were diluted to a concentration of 1×10^8 vp/ml in cDMEM media ± 8 μg/ml FX. Virus ± FX in 1.0 ml of cDMEM were added to each well and incubated at 4°C for 1 hour. The cells were washed twice with 2.0 ml of cDMEM and resuspended in 1.0 ml cDMEM. Viral and total genomic DNA were isolated using a DNAeasy Mini Spin Kit (QIAGEN, Crawley, UK) and quantified by NanoDrop (ND-1000 spectrophotometer [Labtech International, Ringmer, UK]). One hundred nanograms of total DNA was subjected to quantitative PCR analysis.

Quantitative PCR of Adenoviruses

Quantitative PCR (qPCR) was performed using an ABI prism 7900HT Sequence detection system (Applied Biosystems, Warrington, UK). HD-Adenovirus genomes were detected using the CMV specific primers: RT-CMV-F (5′-CAAGTGTATCATATGCCAAGTACGCCCC -3′) and RT-CMV-R (5′-CCCCGTGAGTCAAACCGCTATCCACGCC-3′). qPCR was done using Power SYBR Green PCR Master Mix, 100 ng of purified total DNA, 3.0 uM primers and the following reaction conditions: 95°C for 15 seconds, 56°C for 15 seconds and 72C for 15 seconds (40 cycles).

DNA Sequencing

DNA sequencing was performed at Mayo Clinic, Advanced Genomics Technology Center, DNA Sequencing Lab. Genbank DNA sequences for DNA polymerase, E1A 13S, fiber, gp19, hexon, L4 partial, terminal protein, and pXi were downloaded and used for primer design and alignment to the previously published Serotype 5 human adenovirus sequence. ABI PRISM Big Dye Terminator Cycle Sequencing Ready Reaction Kit with AmpliTaq® DNA Polymerase, FS was used for sequence reactions. Sequence data was analyzed using the ABI PRISM 3730xl DNA Analyzer. Sequences were edited and a contig from the aligned sequences were created using Sequencher. Sequencing was performed

unidirectionally except in cases of sequence ambiguity or disruption of reading frames when both strands were sequenced. The full-length Ad6 genome can be found at Genbank accession HQ413315.

Phylogenetics of Whole Adenovirus Genomes

The Ad6 genomic DNA sequence was compared to the 34 adenovirus sequences that were available as full-length viral sequences in GenBank. Sequences were aligned by using the Clustal X program (Thompson, Higgins, and Gibson, 1994). All aligned sequences were then inspected manually to correct for apparent mistakes. Positions containing gaps or ambiguously aligned positions were removed from the datasets. Phylogenetic analysis was performed using MrBayes 3.1.2 Software. The Markov Chain Monte Carlo method of Bayesian inference was used to calculate posterior probabilities until a stable likelihood value of $\leqq 0.01$ (Huelsenbeck et al., 2001). The following parameters were used in the setup and analysis of the Ad genomes: Nucleotide model= 4by4, nst=General Time Reversible, Rates=Gamma, nruns=2, Ngen= 1,000,000, Sample frequency=100, mcmdiagn=yes, diagnfreq=1,000, and starting tree=random. Trees were viewed using TreeView v1.6.6. Individual protein alignments were performed with MacVector.

Results

In Vivo Expression of Luciferase

In vivo transduction by intramuscular (i.m.) and intravenous (i.v.) routes has previously been compared between first generation Ad5 (FG-Ad5) and helper-dependent Ad5 (HD-Ad5) by luciferase imaging and vaccination against HIV-1 envelope (Weaver et al., 2009a). HD-Ad1, 2, 5, and 6 have also been compared *in vivo* in mice, but only by monitoring their ability to generate antibodies against HIV-1 envelope in mice and macaques after i.m. injection (Weaver et al., 2009a). Given this, we compared the ability of each of these HD-Ad serotypes to transduce by i.m. and i.v. routes in BALB/c mice by luciferase imaging (Fig. 1).

Groups of 5 mice were administered 10^{10} virus particles (vp) of each HD-Ad serotype carrying the GFP-Luciferase transgene. Luciferase images were taken one day after injection. No differences in overall expression in the muscles by all HD-Ad serotypes after i.m. injection. Interestingly, only HD-Ad6-injected mice showed expression in the liver suggesting leak of virus into the blood and subsequent infection of hepatocytes. When luciferase activity was quantitated, there were no significant differences observed in luciferase expression by any HD-Ad serotype in the muscles (Fig. 2A). In contrast, i.v. injection resulted in significant differences in expression levels. HD-Ad6 produced greater luciferase expression in the liver as compared to HD-Ad1, HD-Ad2, and HD-Ad5 (Fig. 1 and 2B). HD-Ad6 luciferase activity was significantly greater than all other species C viruses where comparison to HD-Ad1, HD-Ad2, and HD-Ad5 gave p values of <0.0001, <0.0001, and <0.001, respectively (Fig. 2B). Conversely, HD-Ad2 showed significantly less luciferase expression than all of the species viruses when compared to HD-Ad1, HD-Ad5, and HD-Ad6 with p values of <0.0001, 0.009, and 0.0006, respectively (Fig. 2B). These data indicate that HD-Ad6 is the most potent species C virus for liver-directed gene therapy in this model and is surprisingly 2, 40, and 100-fold better than HD-Ad5, HD-Ad1, and HD-Ad2.

Factor X-mediated Virus Transduction *In Vitro*

Recent studies have shown that Ad5 binds vitamin K-dependent blood factors including Factor X (FX) to efficiently infect hepatocytes (Parker et al., 2006; Shayakhmetov et al., 2005). To test the effect of FX on the species C viruses, each virus was incubated with and without physiological concentrations of FX (10 μg/ml). This mixture was then added to

human HepG2 hepatocellular carcinoma cells for 1 hour at 4°C and cells were lysed and viral genomes were quantitated by quantitative realtime PCR (Fig. 3A). Under these conditions, all viruses bound the cells better in the presence of FX, however the fold increase in binding was weakest for HD-Ad1. To test functional infection, HepG2 and SKOV-3 ovarian carcinoma cells with low Coxsackie and Adenovirus Receptor (CAR) expression were infected with the viruses with and without prior FX incubation for one hour, cells were washed and luciferase activity was measured 24 hours later (Fig. 3B and C). FX significantly increased luciferase expression in HepG2 cells by HD-Ad2, HD-Ad5 and HD-Ad6. FX did not increase luciferase expression by HD-Ad1 in HepG2 cells (Fig. 3B). Similarly, HD-Ad2, HD-Ad5 and HD-Ad6 expression levels were significantly increased in SKOV-3 cells by the addition of FX while expression by HD-Ad1 was not (Fig. 3C).

Ad6 Genome Sequence

Given the higher liver transduction of Ad6 (Fig. 1) and a lack of full genome sequence in Genbank at the time, genomic DNA from wild-type Ad6 (Tonsil 99) was sequenced. Existing Genbank sequences for Ad6 were used along with primer walking to sequence the genome. Seventy-two primers were designed and used to completely sequence the full-length Ad6 genomic. All sequences were aligned in Sequencher and a consensus sequence from the contig was created to obtain the Ad6 genomic DNA sequence.

Phylogenetic Analysis of Ad6 Genomic DNA

In most cases, individual viral proteins are aligned to assess adenovirus phylogeny. Phylogenetic analysis using the entire genome allows for a more complete determination of genetic relativity. This analysis encompasses viral evolution in the presence and absence of selective pressures, such as cross-reactive immunological neutralization. Therefore, this analysis establishes a much more definitive relationship of virus ancestry. Based on this, the full viral genomes of Ad1, 2, 5, and 6 were aligned to the 34 full adenovirus genomes that were available in Genbank using ClustalX. Gaps were removed and the alignments were subjected to Bayesian Inference analysis using MrBayes. Figure 4 shows the phylogenetic tree created by the Markov Chain Monte Carlo analysis that uses posterior probabilities modeling. One million trees were created and 10,000 trees were sampled. As expected, Ad1, 2, 5, and 6 clustered together confirming their association as species C adenoviruses. Full genome comparison determined that Ad6 is most closely related to Ad2 with 98% homology at the DNA as determined by Identity Matrix. In contrast, Ad6 and Ad1 clustered together. These data confirmed the sequence separation of species C viruses from other human Ad species. However, full genome sequence comparisons did not correlate to the statistically significant differences in liver tropism mediated by these vectors (Fig. 1).

Ad6 Genome Organization and Homology to Ad5

Sequences were edited and a contiguous sequence was generated from the aligned sequences using Sequencher. The final Ad6 genomic DNA sequence was characterized by open reading frame analysis, protein translation and viral queries of GenBank Viral Database sequences. The genome organization of Ad6 is shown in Figure 5B and was very similar to other species C adenoviruses. When Ad5 and Ad6 genomic DNAs were aligned, significant differences were found in structural proteins hexon and fiber and in the E3 immune-evasion locus (Fig. 5A). The HD-Ad vectors do not express E3 under the conditions tested (Figs. 1–3). Therefore differences in E3 were not analyzed below.

Species C Fiber Protein Sequence Alignments

Of the variant Ad sequences, only hexon and fiber proteins are packaged in HD-Ad vectors and are relevant to changes in transduction observed in Fig. 1. Fiber is important in the virus

life cycle due to its role in binding to species C Ad receptor CAR. Fiber is also targeted by neutralizing antibodies, although most neutralization occurs on the hexon protein. Given its pivotal role and the higher liver transduction by Ad6, we compared the Ad6 fiber protein sequence to those of the other species C Ads (Fig. 6). Alignment of the fibers indicated that Ad1 and 5 were most similar to each other (Fig. 6A). Were fiber to be the primary determinant of liver tropism, one would expect that Ad1 and 5 might be most similar and both would be most different from the weaker virus Ad2. Since this did not correlate, this suggested that differences in fiber proteins probably do not explain differences in liver pharmacology.

The most notable difference in the fiber proteins was that the Ad6 fiber was substantially shorter than the other species C viruses (Fig. 6B). The fibers from Ad1, Ad2 and A5 fibers were 582, 582 and 581 amino acids, respectively. In contrast, the Ad6 fiber was only 547 amino acids. This 35 amino acid deletion was present in the shaft regions of the fiber that determines the length of the fiber trimer. In contrast to Ad1, 2, and 5 fibers that have 21 - turn repeats, Ad6 fiber had only 18 repeats and appeared to be missing repeats 15, 16, and 17. This was surprising as all species C viruses are generally assumed to be quite similar. Individual amino acids implicated in CAR binding were generally conserved, with the exception of lysine (K) 420 in Ad2. The tail domains used for docking into penton base were entirely conserved between the viruses consistent with the conservation of penton base itself. From this, no overt sequence variations explained the rank order of liver transduction by the species C Ads. While Ad6 does have a uniquely shorter shaft, this was not present in Ad5 that was nearly as efficient as Ad6 *in vivo.* In addition, the Ad6 fiber did not appear to increase virus binding or transduction of CAR-expressing HepG2 cells, suggesting that this truncation is not likely to be involved in increased hepatotropism.

Species C Penton Base Protein Sequence Alignments

In addition to fiber, penton base is known to mediate direct interactions with cellular v integrins via its RGD motif (Wickham et al., 1993). Comparison of the species C penton base proteins revealed little variation in their sequences, particularly in the region including and flanking the RGD peptide (Fig. 7). The only amino acid variation that segregated with Ad5 and 6 as versus Ad1 and 2 was at position 458. This residue is buried in the penton base protein (Liu et al.). Therefore, it is it is not obvious that this change would affect viral hepatotropism.

Species C Hexon Protein Sequence Alignments

In addition to fiber, hexon was the only variant Ad protein that is packaged in HD-Ad vectors. Ad6 hexon consisted of 963 amino acids and with the expected 7 hypervariable regions (HVRs) that are present in all Ads (Fig. 8). Clustal Distance analysis indicated that Ad6 hexon is most closely related to Ad5 hexon consistent with the higher liver transduction observed by these two viruses (Fig. 1). All of the species C viruses retained glutamic acid 451 (E451) in HVR7 that is conserved in all FX-binding Ads (Alba et al., 2009). This is consistent with the observed use of FX by all of the viruses (Fig. 3).

Since almost all variation in the hexons was focused in the HVRs of the viruses, each HVR was individually aligned for all the viruses by Clustal to determine if any of these variations correlated with changes in liver transduction (Fig. 9). HVR 2 and 6 clustered together for the low liver transducing Ad1 and 2 viruses. HVRs 1 and 4 clustered for the high liver-expressing Ad5 and 6 viruses. The most obvious difference between Ad6 and 5 as compared to Ad1 and 2 was that the long, highly charged HVR1 of Ad1 and 2 were 4 to 9 amino acids longer than those of Ad6 and 5. These comparisons suggest that liver transduction by the

species C viruses may be mediated by differences in hexon proteins rather than by changes in the fiber protein.

Discussion

Species C Ads are thought to be the most well-understood adenovirus families in use based in large part on the vast array of information that is available for Ad5 and to a lesser extent for Ad2. While it is true that the species C viruses do share a high degree of sequence homology, direct comparisons between the biologies of these viruses *in vivo* suggest that where differences do occur, they can fundamentally impact virus biology.

In this work, we compared the ability of HD-Ad vectors packaged with Ad1, 2, 5, and 6 viral capsids after i.m. and i.v. injection. We surprisingly found nearly 40-fold differences in liver transduction after i.v. injection by these family members. Ad2 was the weakest virus and Ad6 was more potent than Ad5. While this data was surprising, it is in part consistent with the few comparisons that were performed previously. For example, previous comparison of HD-Ad2 and HD-Ad5 noted that both were effective at liver gene therapy (Parks, Evelegh, and Graham, 1999). However, when the data is examined closely, it actually shows that Ad2 mediated 2 to 10-fold lower b-galactosidase activity in the livers of mice than Ad5 after i.v. injection.

Given that the HD-Ad vectors that were tested do not encode any Ad genes, differences in tropism must be seated in the major or minor proteins that are encapsidated in the vectors. Sequence comparison of Ad5 and Ad6 showed that most variation is in the major capsid proteins hexon and fiber. Phylogenetic comparisons of the four viruses did not correlate high liver transduction with variations in fiber protein. Instead, hexon variation appeared more closely associated with the high or low liver transduction phenotype. This correlation is consistent with recent data from our laboratory showing that replacement of the HVRs of Ad5 with the HVRs of Ad6 increases hepatocyte transduction up to 50-fold in mouse and hamster models (Khare and et.al., 2010). This effect appears to be due to reduced recognition by Kupffer cells by Ad6 HVRs than Ad5. Given that only HVR regions were swapped, this provides strong evidence in support of the phylogenic comparison implicating hexon in determining liver tropism differencs for species C Ads. In particular, HVR1 appears to be a promising candidate for this phenotype given its high charge (31 negative and 17 positive charges in Ad5 HVR 1, Fig. 1) and that scavenger receptors on Kupffer cells are thought to recognize charge clusters.

While fiber variations were not consistent with differences in liver tropism, it was surprising to find that the Ad6 fiber was three repeats shorter than the other species C fibers. Previous work with very short fibers from Ad35 with 8 repeats has shown that short-shafted fibers are generally less efficient than long-shafted fibers at infection (Shayakhmetov and Lieber, 2000). Luciferase imaging with the HD-Ads did not indicate any reduced transduction in these mouse studies by Ad6. However, previous comparisons of HD-Ad1, 2, 5, and 6 as vaccines showed that Ad6 generated the weakest anti-HIV envelope antibodies of the four after i.m. injection (Weaver et al., 2009a). Under these conditions, HD-Ad1 generated the strongest antibody responses, Ad2 and 5 intermediate, and Ad6 approximately 50% the antibody levels of Ad1 in mice. Considering that Ad6 is naturally lower seroprevalence, it is possible that slight reductions in CAR-dependent infectivity might make it less efficient at spreading in humans.

In summary, this work has observed surprising phenotypic variations in a family of adenoviruses that have historically been thought to be quite similar. Small percent changes in virus sequence translate in 40-fold differences in hepatotropism. These phenotypic effects

appear to be mediated by changes in the protein sequence of the major capsid protein hexon of Ad. Reducing these interactions with Kupffer cells and hepatocytes holds promise for optimizing Ad vectors to evade the liver for systemic therapy (Alba et al., 2009; Doronin et al., 2009; Fisher et al., 2001; Green et al., 2004; Shashkova et al., 2009). Likewise, modulating these interactions to evade Kupffer cells while maintaining hepatocyte tropism hold promise for use of Ad for liver-directed gene therapy (Croyle et al., 2005; Khare and et.al., 2010; Mok et al., 2005).

Acknowledgments

We would like to thank Shannon May and Mary Barry for their helpful technical assistance. This work was supported by a grant to M.A.B. from NIH (R01-CA136945) and a pilot project to M.A.B. from NIH P50 CA91956 Prostate Cancer SPORE at Mayo Clinic. This work was also supported by a grant to P.N. from NIH (R01-DK067324).

References

Abbink P, Lemckert AA, Ewald BA, Lynch DM, Denholtz M, Smits S, Holterman L, Damen I, Vogels R, Thorner AR, O'Brien KL, Carville A, Mansfield KG, Goudsmit J, Havenga MJ, Barouch DH. Comparative seroprevalence and immunogenicity of six rare serotype recombinant adenovirus vaccine vectors from subgroups B and D. J Virol 2007;81(9):4654–63. [PubMed: 17329340]

Alba R, Bradshaw AC, Parker AL, Bhella D, Waddington SN, Nicklin SA, van Rooijen N, Custers J, Goudsmit J, Barouch DH, McVey JH, Baker AH. Identification of coagulation factor (F)X binding sites on the adenovirus serotype 5 hexon: effect of mutagenesis on FX interactions and gene transfer. Blood 2009;114(5):965–71. [PubMed: 19429866]

Capone S, Meola A, Ercole BB, Vitelli A, Pezzanera M, Ruggeri L, Davies ME, Tafi R, Santini C, Luzzago A, Fu TM, Bett A, Colloca S, Cortese R, Nicosia A, Folgori A. A novel adenovirus type 6 (Ad6)-based hepatitis C virus vector that overcomes preexisting anti-ad5 immunity and induces potent and broad cellular immune responses in rhesus macaques. J Virol 2006;80(4):1688–99. [PubMed: 16439526]

Croyle MA, Le HT, Linse KD, Cerullo V, Toietta G, Beaudet A, Pastore L. PEGylated helper-dependent adenoviral vectors: highly efficient vectors with an enhanced safety profile. Gene Ther 2005;12(7):579–87. [PubMed: 15647765]

D'Ambrosio E, Del Grosso N, Chicca A, Midulla M. Neutralizing antibodies against 33 human adenoviruses in normal children in Rome. J Hyg (Lond) 1982;89(1):155–61. [PubMed: 7096999]

Doronin K, Shashkova EV, May SM, Hofherr SE, Barry MA. Chemical modification with high molecular weight polyethylene glycol reduces transduction of hepatocytes and increases efficacy of intravenously delivered oncolytic adenovirus. Hum Gene Ther 2009;20(9):975–88. [PubMed: 19469693]

Fisher KD, Stallwood Y, Green NK, Ulbrich K, Mautner V, Seymour LW. Polymer-coated adenovirus permits efficient retargeting and evades neutralising antibodies. Gene Ther 2001;8(5):341–8. [PubMed: 11313809]

Garnett CT, Talekar G, Mahr JA, Huang W, Zhang Y, Ornelles DA, Gooding LR. Latent species C adenoviruses in human tonsil tissues. J Virol 2009;83(6):2417–28. [PubMed: 19109384]

Green NK, Herbert CW, Hale SJ, Hale AB, Mautner V, Harkins R, Hermiston T, Ulbrich K, Fisher KD, Seymour LW. Extended plasma circulation time and decreased toxicity of polymer-coated adenovirus. Gene Ther 2004;11(16):1256–63. [PubMed: 15215884]

Hofherr SE, Shashkova EV, Weaver EA, Khare R, Barry MA. Modification of adenoviral vectors with polyethylene glycol modulates in vivo tissue tropism and gene expression. Mol Ther 2008;16(7):1276–82. [PubMed: 18461056]

Huelsenbeck JP, Ronquist F, Nielsen R, Bollback JP. Bayesian inference of phylogeny and its impact on evolutionary biology. Science 2001;294(5550):2310–4. [PubMed: 11743192]

Khare R, et al. Increased Liver Gene Therapy by a Kupffer Cell-evading Adenovirus Vector. Molecular Therapy in review. 2010

Lemckert AA, Sumida SM, Holterman L, Vogels R, Truitt DM, Lynch DM, Nanda A, Ewald BA, Gorgone DA, Lifton MA, Goudsmit J, Havenga MJ, Barouch DH. Immunogenicity of heterologous prime-boost regimens involving recombinant adenovirus serotype 11 (Ad11) and Ad35 vaccine vectors in the presence of anti-ad5 immunity. J Virol 2005;79(15):9694–701. [PubMed: 16014931]

Liu H, Jin L, Koh SB, Atanasov I, Schein S, Wu L, Zhou ZH. Atomic structure of human adenovirus by cryo-EM reveals interactions among protein networks. Science 329(5995):1038–43. [PubMed: 20798312]

Mok H, Palmer DJ, Ng P, Barry MA. Evaluation of polyethylene glycol modification of first-generation and helper-dependent adenoviral vectors to reduce innate immune responses. Mol Ther 2005;11(1):66–79. [PubMed: 15585407]

Palmer D, Ng P. Improved system for helper-dependent adenoviral vector production. Mol Ther 2003;8(5):846–52. [PubMed: 14599819]

Parker AL, Waddington SN, Nicol CG, Shayakhmetov DM, Buckley SM, Denby L, Kemball-Cook G, Ni S, Lieber A, McVey JH, Nicklin SA, Baker AH. Multiple vitamin K-dependent coagulation zymogens promote adenovirus-mediated gene delivery to hepatocytes. Blood 2006;108(8):2554–61. [PubMed: 16788098]

Parks R, Evelegh C, Graham F. Use of helper-dependent adenoviral vectors of alternative serotypes permits repeat vector administration. Gene Ther 1999;6(9):1565–73. [PubMed: 10490766]

Piedra PA, Poveda GA, Ramsey B, McCoy K, Hiatt PW. Incidence and prevalence of neutralizing antibodies to the common adenoviruses in children with cystic fibrosis: implication for gene therapy with adenovirus vectors. Pediatrics 1998;101(6):1013–9. [PubMed: 9606228]

Senac JS, Doronin K, Russell SJ, Jelinek DF, Greipp PR, Barry MA. Infection and killing of multiple myeloma by adenoviruses. Hum Gene Ther 21(2):179–90. [PubMed: 19788385]

Shashkova EV, May SM, Barry MA. Characterization of human adenovirus serotypes 5, 6, 11, and 35 as anticancer agents. Virology 2009;394(2):311–20. [PubMed: 19765790]

Shashkova EV, May SM, Doronin K, Barry MA. Expanded anticancer therapeutic window of hexon-modified oncolytic adenovirus. Mol Ther 2009;17(12):2121–30. [PubMed: 19755961]

Shayakhmetov DM, Gaggar A, Ni S, Li ZY, Lieber A. Adenovirus binding to blood factors results in liver cell infection and hepatotoxicity. J Virol 2005;79(12):7478–91. [PubMed: 15919903]

Shayakhmetov DM, Lieber A. Dependence of adenovirus infectivity on length of the fiber shaft domain. J Virol 2000;74(22):10274–86. [PubMed: 11044071]

Thompson JD, Higgins DG, Gibson TJ. Improved sensitivity of profile searches through the use of sequence weights and gap excision. Comput Appl Biosci 1994;10(1):19–29. [PubMed: 8193951]

Vogels R, Zuijdgeest D, van Rijnsoever R, Hartkoorn E, Damen I, de Bethune MP, Kostense S, Penders G, Helmus N, Koudstaal W, Cecchini M, Wetterwald A, Sprangers M, Lemckert A, Ophorst O, Koel B, van Meerendonk M, Quax P, Panitti L, Grimbergen J, Bout A, Goudsmit J, Havenga M. Replication-deficient human adenovirus type 35 vectors for gene transfer and vaccination: efficient human cell infection and bypass of preexisting adenovirus immunity. J Virol 2003;77(15):8263–71. [PubMed: 12857895]

Weaver EA, Nehete PN, Buchl SS, Senac JS, Palmer D, Ng P, Sastry KJ, Barry MA. Comparison of replication-competent, first generation, and helper-dependent adenoviral vaccines. PLoS One 2009a;4(3):e5059. [PubMed: 19333387]

Weaver EA, Nehete PN, Nehete BP, Buchl SJ, Palmer D, Montefiori DC, Ng P, Sastry KJ, Barry MA. Protection against Mucosal SHIV Challenge by Peptide and Helper-Dependent Adenovirus Vaccines. Viruses 2009b;1(3):920–938. [PubMed: 20107521]

Wickham TJ, Mathias P, Cheresh DA, Nemerow GR. Integrins avb3 or avb5 promote adenovirus internalization but not virus attachment. Cell 1993;73:309–319. [PubMed: 8477447]

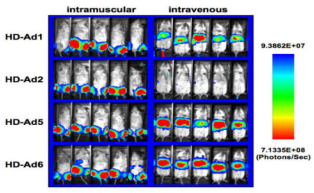

Figure 1.

In vivo luciferase activity induced by HD-Adenovirus. The HD-Ad genome expressing eGFP fused to luciferase was packaged by serotype 1, 2 5, and 6 helper-viruses. Groups of 5 mice were administered 10^{10} vp of the indicated vectors by the intramuscular or intravenous route. 24 hours later the animals were anesthetized, injected with luciferin, and imaged for luciferase activity.

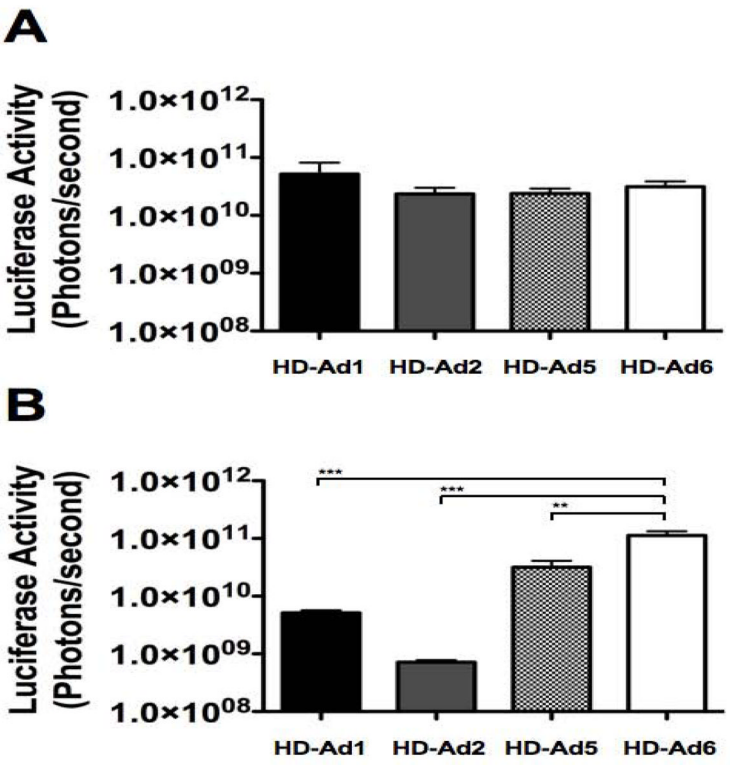

Figure 2.

Quantitation of in vivo luminescence. Groups of 5 mice were injected with 10^{10} vp of the indicated HD-Ad by the intramuscular (A) or intravenous (B) route. Sum luminescence intensities were determined using the Lumazone imaging system software. Error bars indicate standard error.

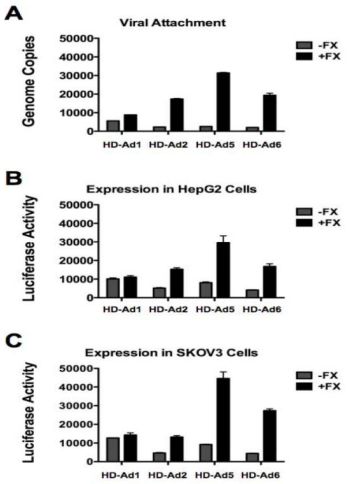

Figure 3.

Effect of FX on binding and transduction on HD-Ad1, 2, 5 and 6 viruses. HD-Ad viruses were incubated with and without FX for 1 hr. at 4 C to determine the effect of FX on HD-Ad cell binding (A). Total DNA was extracted and measured using qPCR. The effect of FX on HD-Ad virus was determined using two cell lines HepG2 (B) and SKOV3 (C). Cells and HD-Ad viruses were incubated with and without FX at 37 °C for 3h. The cells were washed twice and luminescence was determined after 72 hrs. Error bars indicate standard error.

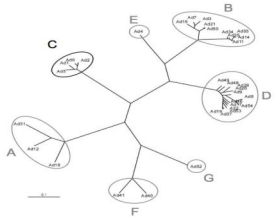

Figure 4.

Bayesian Inference Phylogeny. Markov chain Monte Carlo (MCMC) analysis of 35 complete Adenovirus genome sequences. Complete genome sequences were downloaded from Genbank and aligned using ClustalX. The alignment was inspected visually and all gaps were removed prior to phylogenetic analysis using MrBayes v3.1. The posterior probability of phylogenetic trees (and other parameters of the substitution model) cannot be determined analytically. Instead, MCMC is used to approximate the posterior probabilities of trees by drawing (dependent) samples from the posterior distribution.

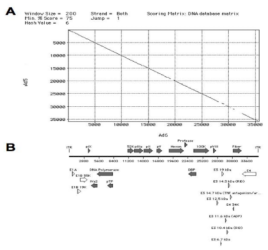

Figure 5.
Identification of comparative differences by sequence alignment analysis. Adenovirus serotypes 5 and 6 were aligned using a Pustell DNA Matrix Analysis tool in MacVector v8.1.1 (A). The complete nucleotide sequence of Ad6 and Ad5 are shown on the X and Y axis, respectively. The diagonal line represents homology and gaps represent non-homologous regions. The relative genomic location of the non-homologous regions is represented below (B).

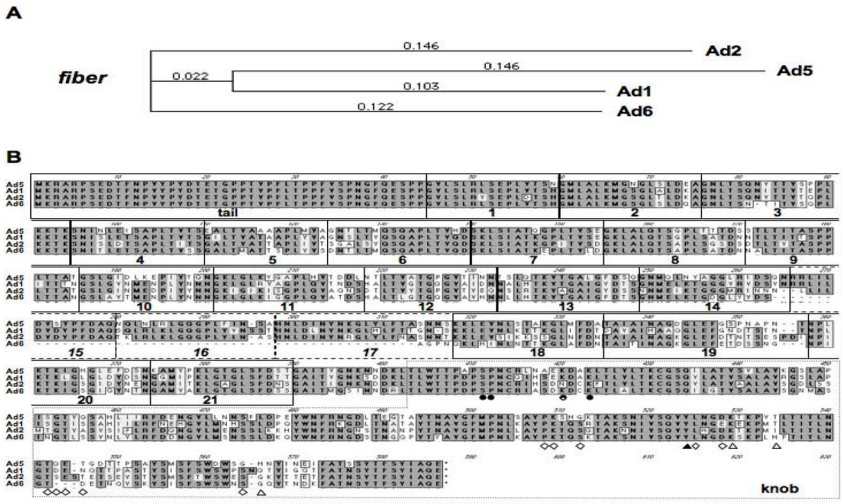

Figure 6.

Fiber sequence comparison. Ad1, 2, 5, and 6 fiber proteins were aligned using ClustalW in macVector v8.1.1. A neighbor-joining tree shows the phylogenetic relationships of the Ad fibers (A). The aligned fiber protein sequences are shown below (B). Boxes over the alignment indicate the location of the fiber tail, fiber shaft repeat motifs, and the fiber knob.

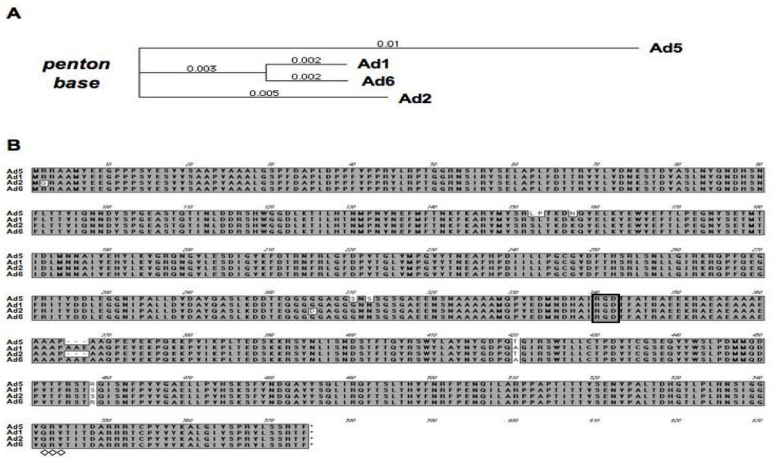

Figure 7.
Penton base sequence comparison. Ad1, 2, 5, and 6 penton proteins were aligned using ClustalW in MacVector v8.1.1. A neighbor-joining tree shows the phylogenetic relationships of the proteins (A). The aligned penton base sequences are shown below (B). The box identifies the RGD motif in each.

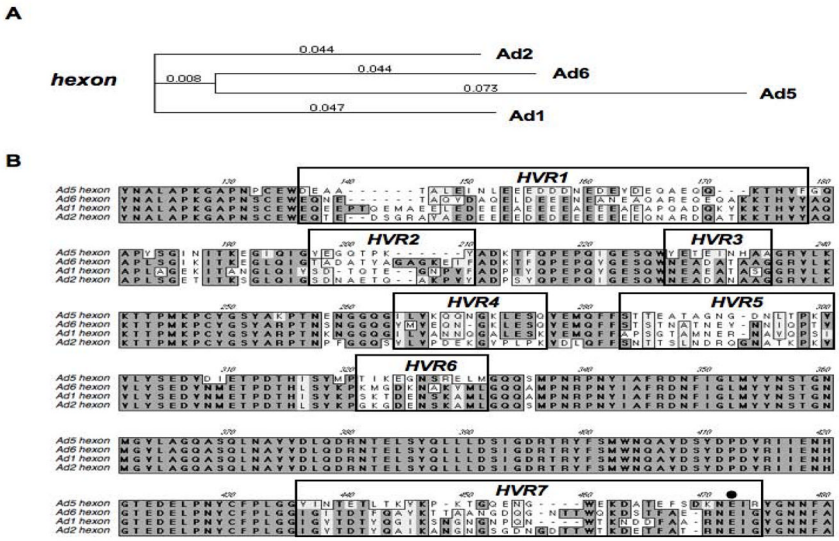

Figure 8.

Hexon sequence comparison. Ad1, 2, 5, and 6 hexon proteins were aligned using ClustalW in MacVector v8.1.1. A neighbor-joining tree shows the phylogenetic relationships of the Ad hexons (A). The aligned hexon protein sequences are shown below (B). Boxes over the alignment indicate the location of the 7 hypervariable regions (HVR1-7).

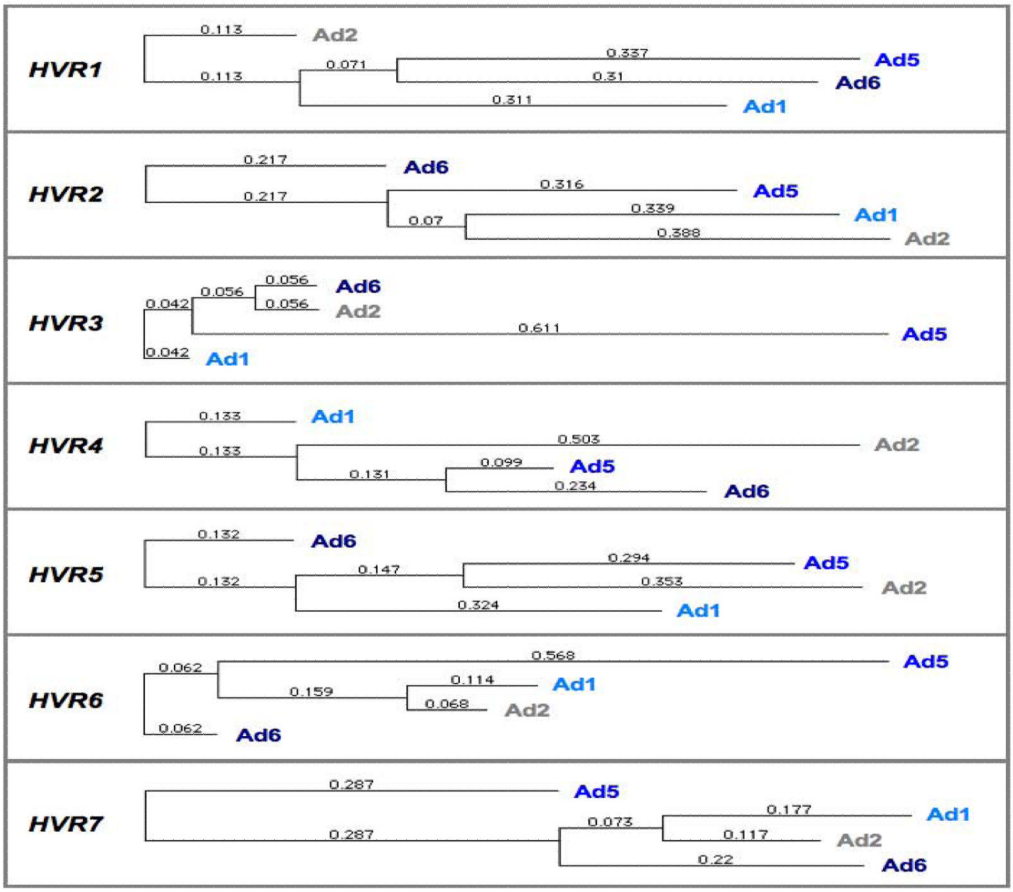

Figure 9.

Gross differences in the genetic relationships of the HVRs between viruses. Neighbor-joining phylogenetic analyses for each HVR were performed. Seven phylogenetic trees represent the genetic distances at each HVR.